Phys. Med. Biol. **56** (2011) 6149–6160 doi:10.1088/0031-9155/56/19/001

Pre- and post-natal exposure of children to EMF generated by domestic induction cookers

Bor Kos[1], Blaž Valič[2], Damijan Miklavčič[1], Tadej Kotnik[1] and Peter Gajšek[2,3]

[1] Laboratory of Biocybernetics, Faculty of Electrical Engineering, University of Ljubljana, Tržaška 25, SI-1000 Ljubljana, Slovenia
[2] Institute of Non-Ionizing Radiation, Pohorskega Bataljona 215, SI-1000 Ljubljana, Slovenia

E-mail: bor.kos@fe.uni-lj.si, damijan.miklavcic@fe.uni-lj.si, tadej.kotnik@fe.uni-lj.si, blaz.valic@inis.si and p.gajsek@inis.si

Received 8 March 2011, in final form 27 July 2011
Published 30 August 2011
Online at stacks.iop.org/PMB/56/6149

Abstract
Induction cookers are a type of cooking appliance that uses an intermediate-frequency magnetic field to heat the cooking vessel. The magnetic flux density produced by an induction cooker during operation was measured according to the EN 62233 standard, and the measured values were below the limits set in the standard. The measurements were used to validate a numerical model consisting of three vertically displaced coaxial current loops at 35 kHz. The numerical model was then used to compute the electric field (E) and induced current (J) in 26 and 30 weeks pregnant women and 6 and 11 year old children. Both E and J were found to be below the basic restrictions of the 2010 low-frequency and 1998 ICNRIP guidelines. The maximum computed E fields in the whole body were 0.11 and 0.66 V m^{-1} in the 26 and 30 weeks pregnant women and 0.28 and 2.28 V m^{-1} in the 6 and 11 year old children (ICNIRP basic restriction 4.25 V m^{-1}). The maximum computed J fields in the whole body were 46 and 42 mA m^{-2} in the 26 and 30 weeks pregnant women and 27 and 16 mA m^{-2} in the 6 and 11 year old children (ICNIRP basic restriction 70 mA m^{-2}).

(Some figures in this article are in colour only in the electronic version)

1. Introduction

Induction cookers (also referred to as induction hobs) are electrical cooking appliances that use intermediate-frequency magnetic fields to heat the cooking vessel directly without heating the contact surface of the appliance itself (Acero *et al* 2010). The magnetic field induces

[3] Author to whom any correspondence should be addressed.

eddy currents in the ferromagnetic base of the cooking vessel and thereby generates heat from resistive losses in the base of the vessel. The induction cookers typically operate in the frequency range between 20 and 100 kHz, and can deliver powers of up to 3.6 kW (Millan *et al* 2010). Their main advantages are rapid cooking times and higher energy efficiency compared to conventional (resistive) and glass-ceramic (infrared) cookers. With decreasing prices, induction cookers are gaining in popularity and up to 300 thousand units yearly are predicted for sale in Europe alone (ICNIRP 1998).

Exposure scenarios could also include children and pregnant women that belong to a particularly sensitive group of users. It is accepted that children are generally more vulnerable than adults to some environmental, physical and chemical influences (Mancini 2004, Grandjean and Landrigan 2006). It is plausible that such vulnerability could also exist for EMFs, although this conjecture has not yet been proven (Kheifets *et al* 2005). In particular, interesting is the case of pregnant women as with the typical position of a mother in front of the cooker, the foetus is at a very small distance to the source of magnetic field. Furthermore, children might also occasionally use domestic cooking appliances and their height would put their heads, and therefore their central nervous system, closer to the field source than adults.

There are as yet few reports available on the subject of human exposure to the magnetic fields generated by induction cookers. Two papers (Stuchly and Lecuyer 1987, Yamazaki *et al* 2004) report measurements of domestic induction cookers and conclude that the fields are below the ICNIRP reference levels. Viellard *et al* (2007) have also reported that measured fields are below the reference levels at 30 cm from the device, as measured according to the EN 62233 standard. However, closer to the devices, the magnetic field approaches and in some operating conditions that can plausibly occur even exceeds the reference levels for magnetic flux density.

In this paper, we present a numerical model of a domestic induction cooker and validate it with measurements. We use the model to perform simulations of induced current density and internal electric field according to the original ICNIRP (1998) and the revised low-frequency ICNIRP (2010) guidelines in two models of pregnant women and in two models of children—a 6 year old male and an 11 year old female.

2. Materials and methods

2.1. Measurement protocol

Two European standards have been published that deal with the measurement procedures for induction cookers: the first one was the CENELEC 50366: *Household and similar electrical appliances—electromagnetic fields—methods for evaluation and measurement* (CENELEC 2003), which was superseded by the IEC 62233: *Measurement methods for electromagnetic fields of household appliances and similar apparatus with regard to human exposure* in 2008 (IEC 2005). Both standards employ a technically equivalent measurement procedure in which the fields are measured at 30 cm from the front of the device in a vertical line. The field should be averaged over an area of 100 cm^2 to ensure that local maxima and inhomogeneities do not affect the measurements excessively. The averaged magnetic flux density in front of the device has to be below the 1998 ICNIRP guidelines reference levels for general public (ICNIRP 1998), which is 6.25 μT for the range from 800 Hz to 150 kHz, which includes all the frequencies used in induction cookers.

The measurement was performed with a calibrated Narda ELT-400 field meter with a 100 cm^2 isotropic probe (both from Narda Safety Test Solutions GmbH, Pfullingen, Germany). The instrument was used in 'field strength' mode, which has a flat frequency response across

a wide frequency range of 1–400 kHz. The analogue output of the ELT-400 was connected to a Tektronix MSO4104 oscilloscope (Tektronix Inc., Beaverton, OR, USA), with the spectrum analysis performed using FFT. According to the currently valid domestic appliance standard (IEC 2005), measurements were performed at 30 cm from the front of the induction cooker, and additionally, the fields were also measured at shorter distances of 1, 5 and 10 cm from the front of the appliance, to enable a better validation of our numerical model. The heating power was set to maximum with the boost function activated. The field meter was mounted on a non-conductive tripod and the height was varied manually. The measurements were taken at 5 cm vertical spacings, from −25 to 45 cm relative to the level of the cooking surface. The measurements were performed with a full pot of water on the largest cooker with a maximum power setting (power-boost function activated). The RMS value of the magnetic flux density (denoted henceforth as B) was recorded in each location. Separately, the frequency spectrum was recorded on the oscilloscope to determine the frequency content and enable adequate comparison with the basic restrictions.

Additionally, we have measured the low-frequency component of B using a calibrated Wandel & Golterman EFA-3 (now Narda Safety Test Solutions GmbH, Pfullingen, Germany) field meter with a B field probe and a low-pass filter with the cut-off frequency set to 3 kHz. The measurements show that the maximum value of B_{RMS} at 1 cm distance was less than 2.2 μT. This justified the exclusion of the ELF component of the magnetic field from the dosimetric simulations, since this value represents less than 2.2% of the reference levels according to the 1998 ICNIRP guidelines and even less than that according to the 2010 guidelines, which have a higher reference level for general public exposure.

The main components of an induction cooker are the induction coils, which are placed below the cooking surface, the ferrite magnetic substrate and the cooking vessel, which acts as a part of the resonance circuit, absorbs the magnetic field energy and converts it into heat (Acero *et al* 2010). Yamazaki *et al* (2004) have developed a method for simple characterization of the magnetic field of an induction cooker by a single magnetic dipole moment (i.e. one that can be modelled by a single current loop), but we opted for a more detailed model consisting of three vertically displaced, concentric current loops. The middle current loop presents the main (source) coil, while the upper and lower current loops, with the currents flowing in a counter-phase to the main loop, present the eddy currents in the base of the pot and in the ferrite flux guides below the main coil, respectively (Koller and Novak 2009). A comparison of such a three-loop model to the simpler single-loop model showed that in the former, the differences between simulations and measurements are smaller, in particular close to the cooker, which is the region of interest for this study (data not shown).

2.2. *Human models*

Two anatomical models of pregnant women were used in the study. The first model was made by our group by combining segmented computed tomography images of a 30 weeks pregnant woman (Shi and Xu 2004) with cross-sectional images of a female from the Visible Human database obtained from cryosection (Ackerman 1998). The original image set of Shi and Xu included only the thoracic region from below the pubic symphysis to above the liver and was extended with homogeneous upper and lower body parts using the iSeg segmenting software (Zurich Med Tech, Zurich, Switzerland). The slice thickness of the model is 7 mm in the central region, and 3 mm in the upper and lower homogeneous parts. The height of the model is 158 cm and the weight is 93 kg, giving body-mass index of 37, which classifies the subject as obese. The total weight of the model is close to the weight of the original subject as reported by Shi and Xu (2004), while the height of the original subject was not reported. The

Table 1. Dielectric properties of foetal tissues used in the simulations.

Tissue	Conductivity	Source
Foetal bladder	0.22	(Gabriel *et al* 1996b)
Foetal gray matter	0.34	(Lu *et al* 1996)
Foetal cerebro-spinal fluid	1.60	(Grimnes and Martinsen 2008)
Foetal eye	1.50	(Gabriel *et al* 1996b)
Homogeneous foetal body	0.44	(Lu *et al* 1996)
Foetal heart	0.65	(Gabriel *et al* 2009)
Foetal lung	0.22	(Lu *et al* 1996)
Foetal stomach	0.54	(Gabriel *et al* 1996b)
Umbilical cord	0.70	(Gabriel *et al* 1996b)
Amniotic fluid	1.50	(Gabriel *et al* 1996b)
Uterus	0.53	(Gabriel *et al* 1996b)
Skeleton of foetus	0.30	(Gabriel *et al* 2009)
Placenta	0.70	(Gabriel *et al* 1996b)

model consists of a total of 29 different tissues, and the utero-foetal unit is segmented into the following tissues: uterus, placenta, homogeneous foetal body and the skeleton of foetus. The volumes of the abdominal organs are realistic. The volume of the liver (2049 cm^3) is larger than average (Dello *et al* 2011), while the volume of the spleen (218 cm^3) is very close to the mean value reported by Spielmann *et al* (2005).

The second pregnant female was built by combining MRI image data (Bibin *et al* 2010) with a homogeneous three-dimensional computer-generated model of a female (Daz 3D Studio, www.daz3d.com). The height of the model is 167 cm and the total weight is 48 kg, giving a body-mass index of 17.

The total weights of the foetuses are 0.92 and 1.48 kg for the 26 and 30 weeks pregnant models, respectively. This is very close to the median values, which are 0.89 and 1.53 kg for 26 and 30 weeks, respectively, according to a formula for foetal weight for the European ethnic group (Gardosi *et al* 1995). While the weight of the foetuses is very near the median, the weight of the mothers is either on the underweight or obese side of the spectrum.

The anatomical models of children were the 6 year old boy and 11 year old girl from the Virtual Family (Christ *et al* 2010). All models were voxelled with a resolution of $2 \times 2 \times 2$ mm^3, to provide a high spatial resolution of the results for extraction.

The electric conductivities of tissues were taken from various sources. The values used for foetal conductivities are shown in table 1. Where available, we used directly measured values for foetal tissues measured at 100 kHz, as reported by Lu *et al* (1996). They measured the values from aborted foetuses after 15 weeks of gestation. For the foetal body, we used the measurements from muscle tissue reported by Lu *et al* (1996). Measurements of the dielectric properties of placenta, amniotic fluid and umbilical cord have been reported recently by Peyman *et al* (2011); however, they measured only at frequencies above 200 MHz. Below this frequency, no such data exist; however, the conductivities of umbilical cord and placenta are close to the conductivity of blood, while the conductivity of amniotic fluid is close to that of cerebrospinal fluid. These values have been used previously at low frequencies (Hand *et al* 2006, Dimbylow 2007).

2.3. Numerical computations

We used the magneto quasi-static low-frequency solver implemented in SEMCAD X v 14.4 (SPEAG, Zurich, Switzerland). The solver is based on the Biot–Savart law

$$\mathbf{A}_0(\mathbf{r}) = \frac{\mu_0}{4\pi} \int_\Omega \frac{\mathbf{j}_0(\mathbf{r}')}{|\mathbf{r} - \mathbf{r}'|} \, \mathrm{d}\mathbf{r}' \tag{1}$$

in which it assumes a constant magnetic permeability μ_0 throughout the domain of integration Ω and computes the vector magnetic potential $\mathbf{A}_0$ generated by the source current $\mathbf{j}_0$. In the lossy domain (i.e. in the regions where electric conductivity σ is nonzero), the electric field $\mathbf{E}$ is then computed from the equation

$$\nabla \cdot (\sigma \mathbf{E}) = -j\omega \nabla \cdot (\sigma \mathbf{A}_0). \tag{2}$$

This equation is obtained from the more general charge continuity equation under the assumption $\sigma \gg \omega\varepsilon$ (where ω is the angular frequency and ε is the dielectric permittivity), which is valid for most body tissues.

2.4. Exposure scenarios

Each model was positioned standing upright with the nearest point of the body being 180 mm from the centre of the cooker, while in the lateral direction, the centres of the cooker and the body were aligned. Vertically, the models were positioned 850 mm lower than the level of the induction cooker, which represents a typical height of domestic kitchen work surfaces, as can be seen in figure 1. This choice of positioning represents an exposure scenario at least

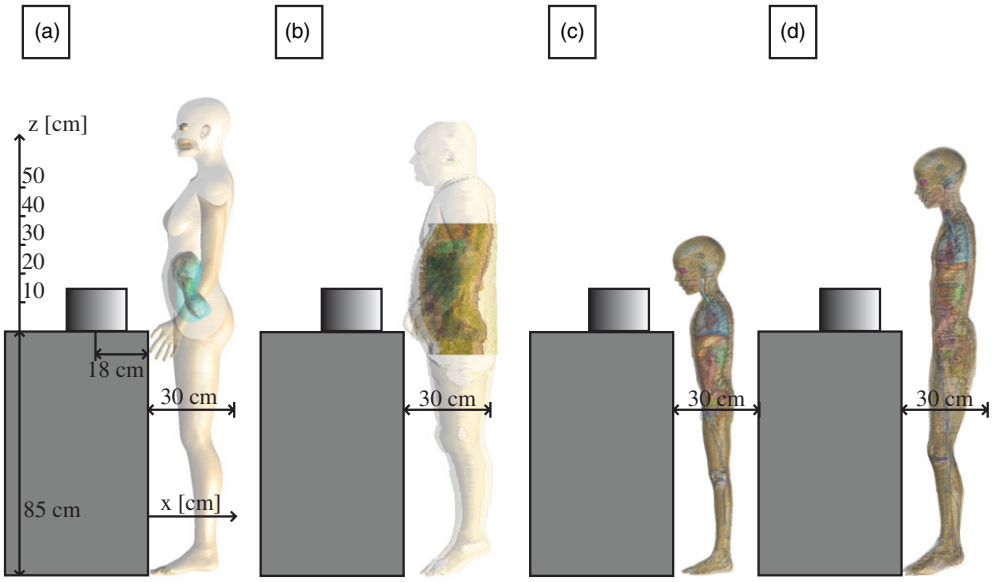

Figure 1. Side view of the exposure setup for the human models. The models are (a) a 50 kg, 26 weeks pregnant female (Bibin *et al* 2010), (b) a 90 kg, 30 weeks pregnant female (Shi and Xu 2004), (c) a 19 kg, 6 year old male (Christ *et al* 2010) and (d) a 36 kg, 11 year old female (Christ *et al* 2010). In all cases, the models are positioned with the feet at floor level, 85 cm lower than the level of cooking surface and with the closest point at 0 cm from the front of the appliance. The heights (z) and distance (x) of measurements corresponding to figure 2 are also indicated.

Table 2. Uncertainty budget of the measurements and numerical dosimetry.

Uncertainty sources	Tolerance (dB)	Distribution	Divisor	c_i	Uncertainty (dB)	Source
Measurements of *B* field						
Reference field source	1.21	N ($k = 2$)	2	1	0.37	Calibration
B-field probe nonlinearity	0.56	R	1.73	1	0.32	Calibration
Probe anisotropy	0.78	R	1.73	1	0.45	Calibration
Probe frequency dependence	1.12	R	1.73	1	0.42	Calibration
Reproducibility	0.5	N ($k = 1$)	1	1	0.5	Estimate
Numerical dosimetry						
Discretization of tissues	2.88	R	1.73	1	1.66	(Bahr *et al* 2007)
Conductivity of tissues	1.93	R	1.73	1	1.12	(Gabriel *et al* 1996a)
Induction cooker model	0.55	R	1.73	1	0.32	Estimate
Total uncertainty ($k = 1$)					2.02	

as realistic as a position at a distance of 30 cm from the source that is used in measurements according to the IEC standard.

2.5. Error analysis and uncertainty budget

The uncertainty of the measurements and simulations was evaluated and an uncertainty budget was prepared, as shown in table 2. The uncertainty contributions of measurements were as follows: the inaccuracy of the reference field source, the probe's nonlinearity, anisotropy, frequency dependence and the reproducibility of the measurement procedure (calibration from an accredited traceable laboratory). The uncertainty contributions of numerical dosimetry were as follows: uncertainty in conductivities of tissues (Gabriel *et al* 1996a), imprecision in discretization of tissues and the accuracy of the cooker model. Thus, the total estimated uncertainty of the results in this paper is 2.02 dB ($k = 1$) and the extended total uncertainty is 4.04 dB. This is still low compared to the variations in fields produced by similar appliances from different manufacturers and from misaligned or improper cookware; these factors can increase the magnetic fields up to a factor of 5 (Viellard *et al* 2007).

3. Results and discussion

3.1. Measurements and model validation

The values computed numerically in free space were averaged over 100 cm^2 to be comparable with the measurements of the Narda ELT-400. The comparison is shown in figure 2. The data show good agreement, particularly along the vertical at a 10 cm horizontal distance from the appliance, where several important regions of the human models are located (vital organs, utero-foetal unit). The difference between measurements and computations can be explained by the constant permeability used by the SEMCAD solver, which does not allow for exact modelling of the ferromagnetic base of the cooking pot and the ferrite flux guides which are normally found below the induction coils to improve the performance. However, the differences between measurements and simulation are much less than the differences in reported emissions from different devices (Viellard *et al* 2007), which means that the results should be applicable to a wide range of appliances.

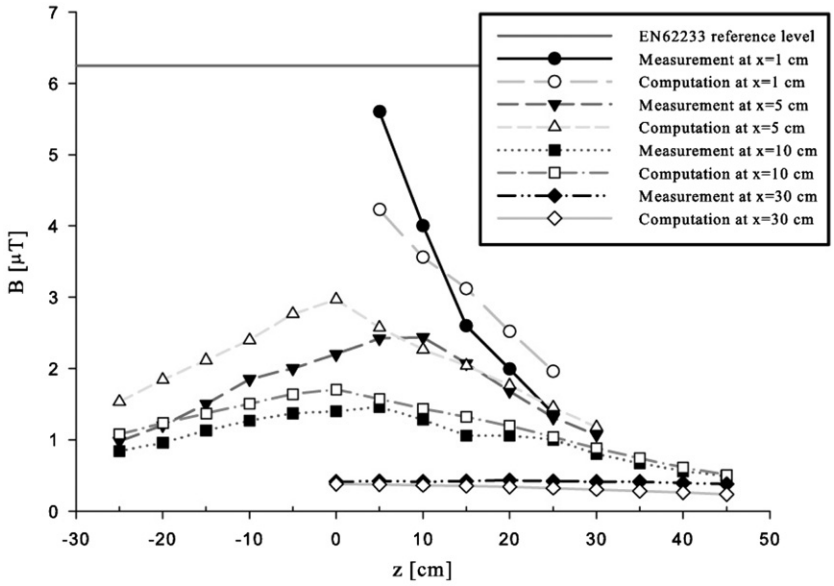

Figure 2. Comparison of the measured and calculated values of the RMS value of B averaged over 100 cm^2 at different heights (z) and horizontal distances from the appliance (x).

Table 3. The spectral content of the B-field up to the fourth odd higher harmonic (all the even harmonics were below the noise level).

Harmonic order	Frequency (kHz)	BRMS (μT)	% of total RMS value[a]
1	35	1.500	99
3	105	0.170	11
5	175	0.082	5
7	245	0.034	2
9	315	0.016	1

[a] Total RMS value at this measurement point was 1.53 μT.

The pot size with respect to the cooking area also has a strong effect on the stray fields. We measured this effect by using pots with diameters of 15, 20 and 25 cm on the same (21 cm) cooking area, and the measured values at a 5 cm horizontal distance from the appliance were 4.5, 2.4 and 0.9 μT, respectively. A misalignment of the pot with respect to the centre of the cooking area increased the measured fields for the 20 and 25 cm pots by up to 20%, while the misalignment of the 15 cm pot did not result in a field increase.

During measurements we also examined the effect of operating several coils of the cooker simultaneously, but operating additional coils did not increase magnetic fields at any distance measured. This could be explained either by a built-in limitation on maximum power draw or by the configuration of resonant inverters, which reduces the maximum delivered power to each coil when several coils are operating simultaneously or increases the maximum power using the so-called 'boost mode' when only one coil is operating (Millan *et al* 2010).

The spectral content of the measured B-field at one of the measurement points is shown in table 3. Based on this measurement, the fundamental and first odd higher harmonics were

used in the computations. The 105 kHz frequency is at the higher end of the frequencies covered by the new (2010) ICNRIP guidelines, so its inclusion is justified.

3.2. Electric field and induced current in the human models

The internal electric fields and induced currents were computed in the four models and are shown in table 4. These results show that the internal electric field is far below the basic restrictions as imposed by the new low-frequency ICNIRP guidelines (2010), while the induced current density is significantly closer to its basic restriction as imposed by the original (1998) ICNIRP guidelines (in the new guidelines the restriction on the induced current density is absent). The only case in which this is not true is the 11 year old child, where the E field is a little less than 50% of the basic restriction. This occurs when low-conductivity voxels (in this case skin) form an electrical connection forming a large loop, which occurs between the hand and thigh in this specific model. The electric field in the low-conductivity region is consecutively very high. Such tissue loops can cause, albeit rarely, serious localized burns in MRI scans (Eising *et al* 2010). In the case of the MRI, however, the burns result from heating from the RF excitation field, which lies in the MHz frequency band. In the cases presented in this work, the internal electric fields are not strong enough to cause any tissue heating. Furthermore, at the frequencies studied in this work, protecting against excessive heating is not the objective of the exposure standards. It remains a question though whether such fields could cause nerve stimulation in areas of conductive tissue loops this large.

The 1998 guidelines specified that the current density should be averaged over an area of 1 cm^2 perpendicular to the current direction, but the averaging was not applied in our computations, as it was previously shown that such averaging is poorly defined and open to conflicting interpretations (Dimbylow 2008, Zoppetti and Andreuccetti 2009). The new low-frequency guidelines specify an averaging volume for an internal electric field of $2 \times 2 \times 2$ mm^3, and in our numerical approach, this was achieved by using a grid with the voxel size identical to the proposed averaging volume. Table 4 also shows data for the 99th percentile value of E and J fields in the central nervous system in the cases of children and in the utero-foetal unit in the cases of the pregnant women, as recommended by ICNIRP (2010). In the whole body, using the 99th percentile would push the estimate too low, the highest per cent accounts for more than 500 g of tissue in the case of the pregnant women. We therefore report the 999th permille, as it gives a more conservative result and is actually comparable between all models used in our study. Figure 3 shows a cross section of E through the centre of the body in all four models.

The induction cooker that was measured, produced less than 0.5 μT at a distance of 30 cm, while the EN 62233 standard allows up to 6.25 μT; therefore, the appliance's magnetic field could be by up to a factor of 12 stronger and still be standard compliant. In comparison with the 1998 ICNRIP guidelines, the 2010 low-frequency guidelines have increased the reference levels for the B-field in the frequency range where the induction cookers operate from 6.25 μT to 27 μT. If the currently valid standard would be revised to the new reference level of 27 μT, and the induction cooker producers would adapt their appliances to this change, the magnetic fields produced by these appliances could be up to a factor of 50 higher.

Our results indicate that the 999th permille (in a $2 \times 2 \times 2$ mm^3 voxel) would exceed the basic restrictions (ICNIRP 2010) if the source magnetic field strength would be increased by a factor of 45; the 999th permille of induced current density would exceed the basic restriction (ICNIRP 1998) if the source magnetic field strength would be increased by a factor of only 2.3. While the E field in the utero-foetal unit and the children's central nervous systems is generally low, and by more than two orders of magnitude below the basic restriction, the 99th percentile

Table 4. The computed values of the electric field (E) and current density (J) in the human models. The maxima are given for the whole body and the UFU (utero-foetal unit) for the pregnant women, and for the whole body and the CNS (central nervous system) in children.

	26 Weeks		30 Weeks		6 year old child		11 year old child	
	E (V m^{-1})	J (mA m^{-2})	E (V m^{-1})	J (mA m^{-2})	E (V m^{-1})	J (mA m^{-2})	E (V m^{-1})	J (mA m^{-2})
Values of dosimetric quantities at 35 kHz								
Max WB	0.111	46	0.660	42	0.281	27	2.280	16
999th permille WB	0.038	27	0.080	18	0.099	14	0.065	10
Max CNS/UFU	0.028	46	0.078	23	0.039	4.4	0.009	1.0
99th centile CNS/UFU	0.024	29	0.032	18	0.021	2.3	0.005	0.54
Percentage of basic restriction[a]								
Max WB	2.3	65	14.0	60	6.0	39	48.2	22
999th permille WB	0.80	39	1.7	25	2.1	20	1.4	15
Max CNS/UFU	0.60	65	1.6	33	0.82	6.3	0.19	1.4
99th centile CNS/UFU	0.52	41	0.68	26	0.43	3.3	0.10	0.8
Values of dosimetric quantities at 105 kHz								
Max WB	0.037	15	0.218	14	0.093	9.0	0.752	5.2
999th permille (WB	0.012	9.1	0.026	5.8	0.017	4.7	0.021	3.4
Max CNS/UFU	0.009	15	0.026	7.7	0.013	1.4	0.003	0.32
99th centile CNS/UFU	0.008	10	0.011	6.1	0.007	0.76	0.002	0.18
Percentage of basic restriction[b]								
Max WB	0.26	7.2	1.54	6.7	0.66	4.3	5.32	2.5
999th permille WB	0.09	4.3	0.19	2.8	0.12	2.2	0.15	1.6
Max CNS/UFU	0.07	7.2	0.18	3.7	0.09	0.69	0.02	0.15
99th centile CNS/UFU	0.06	4.5	0.07	2.9	0.05	0.36	0.01	0.09
Combined percentage of basic restriction								
Max WB	2.6	72	16	67	6.6	43	54	25
999th permille WB	0.89	44	1.9	28	2.2	23	1.5	16
Max CNS/UFU	0.67	72	1.8	37	0.91	7.0	0.21	1.6
99th centile CNS/UFU	0.57	46	0.75	29	0.48	3.7	0.11	0.86

[a]At 35 kHz, basic restriction for E is 4.725 V m^{-1} and for J it is 70 mA m^{-2}.
[b]At 105 kHz, basic restriction for E is 14.175 V m^{-1} and for J it is 210 mA m^{-2}.

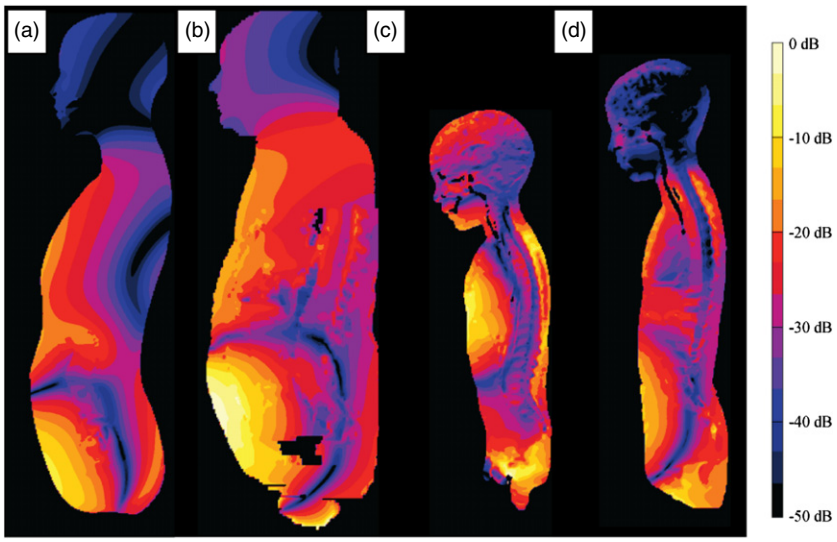

Figure 3. A cross section showing the *E* field values through the centre of the body. 0 dB represents 0.1 V m^{-1}. The models are (a) 26 weeks pregnant, (b) 30 weeks pregnant, (c) 6 year old child and (d) 11 year old child.

of the *J* field in the utero-foetal unit is relatively high, being only by a factor of 2.2 below the basic restrictions. These high values are located in the placenta in the case of 30 weeks pregnant and in the amniotic fluid in the case of 26 weeks pregnant. Taking into account the estimated extended ($k = 2$) uncertainty, and the measured variation between different pots, the 95% confidence interval of the computed internal electric field spans the range from 0.2% up to 6% of the ICNIRP 2010 basic restrictions, while for the induced current density it spans the range from 3.8% up to 130% of the (now obsolete) ICNIRP 1998 basic restrictions. These confidence intervals can also realistically include the variations in fields produced by different appliance models.

4. Conclusions

The results show that the magnetic fields produced by induction cookers do not cause the basic restriction for the internal electric field (ICNRIP 2010) to be exceeded in children and foetuses, even when the fields are increased by a factor of 5. Such an increase can realistically happen when the cookware is inappropriate for use on induction cookers and/or miss-aligned. Maximum exposure of a foetus is less than 2% of the new ICNIRP guidelines for limiting exposure to low-frequency electromagnetic fields, which makes exceeding the basic restriction unlikely. Furthermore, the 999th permille of the internal electric field in the whole body was less than 2.2% of the basic restriction in all cases, including children's central nervous system. The induced current density, however, is closer to its respective basic restriction (ICNIRP 1998) than the electric field and could exceed the basic restrictions even for induction cookers in compliance with the currently valid EN 62233 standard.

Acknowledgments

The research was funded by the Slovenian Research Agency under various grants. The authors would like to thank Dr Xu of the Rensselaer Polytechnic Institute for providing us with the images of the 30 weeks pregnant woman.

References

Acero Jesus, Burdio J, Barragan L, Navarro D, Alonso R, Ramon J, Monterde F, Hernandez P, Llorente S and Garde I 2010 Domestic induction appliances *IEEE Ind. Appl. Mag.* **16** 39–47

Ackerman M J 1998 The Visible Human Project *Proc. IEEE* **86** 504–11

Bahr A, Bolz T and Hennes C 2007 Numerical dosimetry ELF: accuracy of the method, variability of models and parameters, and the implication for quantifying guidelines *Health Phys.* **92** 521

Bibin L, Anquez J, de la Plata Alcalde J P, Boubekeur T, Angelini E D and Bloch I 2010 Whole-body pregnant woman modeling by digital geometry processing with detailed uterofetal unit based on medical images *IEEE Trans. Biomed. Eng.* **57** 2346–58

CENELEC 2003 *EN 50366:2003 Household and Similar Electrical Appliances. Electromagnetic Fields. Methods for Evaluation and Measurement* (Brussels: CENELEC)

Christ A *et al* 2010 The Virtual Family—development of surface-based anatomical models of two adults and two children for dosimetric simulations *Phys. Med. Biol.* **55** N23–38

Dello S A W G, Stoot J H M B, van Stiphout R S A, Bloemen J G, Wigmore S J, Dejong C H C and van Dam R M 2011 Prospective volumetric assessment of the liver on a personal computer by nonradiologists prior to partial hepatectomy *World J. Surg.* **35** 386–92

Dimbylow P J 2007 SAR in the mother and foetus for RF plane wave irradiation *Phys. Med. Biol.* **52** 3791–802

Dimbylow P J 2008 Quandaries in the application of the ICNIRP low frequency basic restriction on current density *Phys. Med. Biol.* **53** 133–45

Eising E G, Hughes J, Nolte F, Jentzen W and Bockisch A 2010 Burn injury by nuclear magnetic resonance imaging *Clin. Imaging* **34** 293–7

Gabriel C, Peyman A and Grant E 2009 Electrical conductivity of tissue at frequencies below 1 MHz *Phys. Med. Biol.* **54** 4863–78

Gabriel S, Lau R and Gabriel C 1996a The dielectric properties of biological tissues: II. Measurements in the frequency range 10 Hz to 20 GHz *Phys. Med. Biol.* **41** 2251–69

Gabriel S, Lau R and Gabriel C 1996b The dielectric properties of biological tissues: III. Parametric models for the dielectric spectrum of tissues *Phys. Med. Biol.* **41** 2271–93

Gardosi J, Mongelli M, Wilcox M and Chang A 1995 An adjustable fetal weight standard *Ultrasound Obstet. Gynecol.* **6** 168–74

Grandjean P and Landrigan P 2006 Developmental neurotoxicity of industrial chemicals *Lancet* **368** 2167–78

Grimnes S and Martinsen O G 2008 *Bioimpedance and Bioelectricity Basics* (Amsterdam: Elsevier)

Hand J W, Li Y, Thomas E L, Rutherford M A and Hajnal J V 2006 Prediction of specific absorption rate in mother and fetus associated with MRI examinations during pregnancy *Magn. Reson. Med.* **55** 883–93

ICNIRP 1998 Guidelines for limiting exposure to time-varying electric, magnetic, and electromagnetic fields (up to 300 GHz) *Health Phys.* **74** 494–522

ICNIRP 2010 Guidelines for limiting exposure to time-varying electric and magnetic fields (1 Hz to 100 kHz) *Health Phys.* **99** 818–36

IEC 2005 *EN 62233: Measurement Methods for Electromangetic Fields of Household Appliances and Similar Apparatus with Regard to Human Exposure* (Geneva: International Electrotechnical Commission)

Kheifets L, Repacholi M, Saunders R and van Deventer E 2005 The sensitivity of children to electromagnetic fields *Pediatrics* **116** e303–13

Koller L and Novak B 2009 Improving the energy efficiency of induction cooking *Electr. Eng.* **91** 153–60

Lu Y, Cui H, Yu J and Mashimo S 1996 Dielectric properties of human fetal organ tissues at radio frequencies *Bioelectromagnetics* **17** 425–6

Mancini A 2004 Skin *Pediatrics* **113** 1114–9

Millan I, Burdio J M, Acero J, Lucia O and Palacios D 2010 Resonant inverter topologies for three concentric planar windings applied to domestic induction heating *Electron. Lett.* **46** 1225–6

Peyman A, Gabriel C, Benedickter H and Frohlich J 2011 Dielectric properties of human placenta, umbilical cord and amniotic fluid *Phys. Med. Biol.* **56** N93–8

Shi C and Xu X G 2004 Development of a 30-week-pregnant female tomographic model from computed tomography (CT) images for Monte Carlo organ dose calculations *Med. Phys.* **31** 2491–7

Spielmann A L, DeLong D M and Kliewer M A 2005 Sonographic evaluation of spleen size in tall healthy athletes *AJR Am. J. Roentgenol.* **184** 45–9

Stuchly M A and Lecuyer D W 1987 Electromagnetic-fields around induction-heating stoves *J. Microw. Power Electromagn. Energy* **22** 63–9

Viellard C, Romann A, Lott U and Kuster Niels 2007 B-field exposure from induction cooking appliances *IT'IS Report* (Zurich: IT'IS Foundation) http://www.bag.admin.ch/themen/strahlung/00053/00673/03156/index.html

Yamazaki K, Kawamoto T, Fujinami H and Shigemitsu T 2004 Equivalent dipole moment method to characterize magnetic fields generated by electric appliances: extension to intermediate frequencies of up to 100 kHz *IEEE Trans. Electromagn. Compat.* **46** 115–20

Zoppetti N and Andreuccetti D 2009 Review of open problems in assessing compliance with 2004/40/EC directive exposure limit values for low-frequency current density by means of numerical techniques *Radiat. Prot. Dosim.* **137** 247–51